Interfacial Structural Crossover and Hydration Thermodynamics of Charged C_{60} in Water: Electronic supplementary information (ESI)

Setare Mostajabi Sarhangi,[1] Morteza M. Waskasi,[2] Seyed Majid Hashemianzadeh,[1] and Dmitry V. Matyushov[3]
[1)] *Molecular Simulation Research Laboratory, Department of Chemistry, Iran University of Science and Technology, Tehran 16846-13114, Iran*
[2)] *School of Molecular Sciences, Arizona State University, PO Box 871504, Tempe, AZ 85287-1504*
[3)] *Department of Physics and School of Molecular Sciences, Arizona State University, PO Box 871504, Tempe, AZ 85287-1504* [a)]

I. SIMULATION PROTOCOL

Gaussian'09[1] was used to optimize the geometry of fullerene in different oxidation states using density functional theory (DFT) with B3LYP functional and the 6-31+g(d) basis set. All atomic partial charges for C_{60} in all charge states were calculated using the CHELPG charge model implemented in Gaussian'09. The atomic charges from the calculations are listed in Table S1.

All simulations were performed with NAMD 2.9 software suite,[2] and VMD software package[3] was used for visualization of the dynamics and the analysis of the molecular dynamics trajectories. The charge distributions of fullerenes in different oxidation states were taken from DFT calculations. The SPCE water was added to the system using the solvate plugin from VMD[3] with some modifications. The C_{60} molecules were hydrated with 2413 water molecules. For all initial systems, a steepest descent minimization was performed for 5000 steps. The NPT/NVT simulations applied Langevin temperature and pressure controls with the following parameters: a damping coefficient of 1 ps, piston period of 200 fs, the piston decay time of 50 fs, the piston target pressure of 1.01325 bar, and constant temperature control set to target temperatures (240, 260, 280, 290, 300, 320, 340 and 360 K).[4]

NPT equilibration was followed by 10 ns NVT equilibration for each redox state. The NVT simulations were performed using the same parameters as the NPT simulations, but removing the constant pressure controls. Box dimensions (43.10 Å× 41.81 Å× 42.98 Å), taken after a short 10 ns NPT run, were held constant throughout all subsequent NVT simulations. NVT simulations, 2 ns each, with the temperature increments of 1 K were used for cooling and heating from the initial temperature of 300 K. The time step of 2.0 fs was adopted for all simulations, and the saving frequency was 200 fs. Simulations with the length of 110 ns were done for temperatures 280, 300 and 320 K. For other temperatures, 30 ns production simulations were carried out. For fullerenes in charge states 0, −1, −2 and −3, the simulation length was 110 ns at all temperatures. Long-range electrostatic interactions were treated with the particle mesh Ewald technique using a cutoff distance of 18.0 Å[3]. The AMBER atom type CA force field was used for the C_{60} atoms in all redox states.

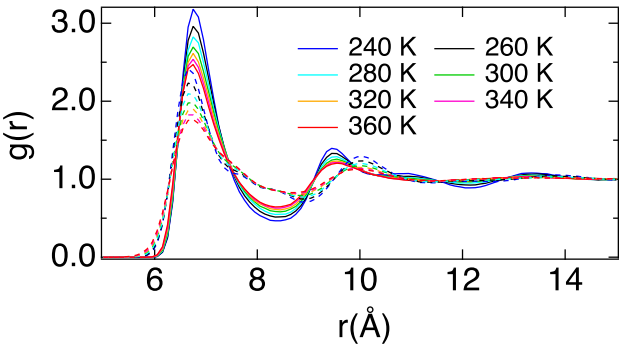

Figure S1. The radial distribution function, $g(r)$, of C_{60}^{+1} between center of fullerene and oxygen (solid lines) and hydrogen (dash lines) of water molecules for last 50 ns of simulation trajectory in different temperatures listed in the plot.

II. RADIAL DISTRIBUTION FUNCTIONS

The calculations of the pair distribution functions (PDFs) are performed on last 50 ns of simulation trajectories. The PDFs are calculated between the center of fullerene and oxygens and hydrogens of waters in the simulation box. The results of calculations are shown in Figs. S1–S6. The radial distribution functions for the hydrogen atoms, $g_{\rm H}(r)$, and for the oxygen atoms, $g_{\rm O}(r)$, were combined to produce the charge density distributions $g_q(r)$ shown in Fig. S7. Those are calculated from the equation

$$g_q(r) = 2q_{\rm H}g_{\rm H}(r) + q_{\rm O}g_{\rm O}(r), \qquad \text{(S1)}$$

where $q_{\rm H}$ and $q_{\rm O}$ are the partial atomic charges of the hydrogen and oxygen atoms in the SPC/E water model.

III. DYNAMICS

The analysis of the hydration shell dynamics was performed for C_{60}^{z} in charge states from $z = +1$ to -4 and

[a)] Electronic mail: dmitrym@asu.edu

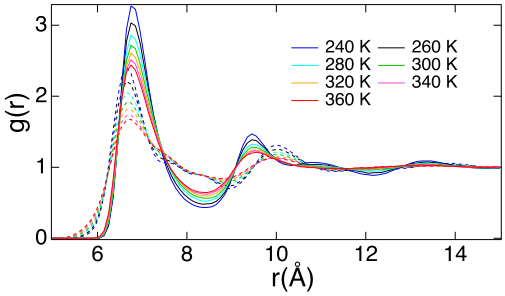

Figure S2. The radial distribution function, $g(r)$, of C_{60}^{0} between center of fullerene and oxygen (solid lines) and hydrogen (dash lines) of water molecules for last 50 ns of simulation trajectory in temperature range 240-360 K.

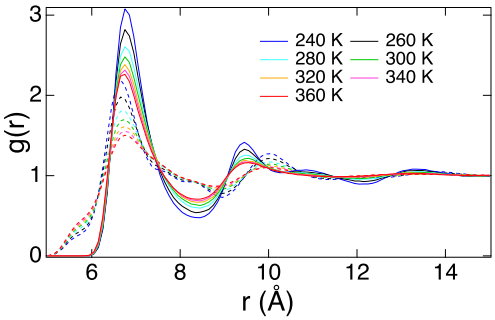

Figure S3. $g(r)$ of C_{60}^{-1} between center of fullerene and oxygen (solid lines) and hydrogen (dash lines) of water molecules for simulation trajectory 60 to 110 ns in temperature range 240-360 K.

temperatures in the range from 240 to 360 K. The orientational order parameters of water molecules in the first hydration shell of fullerene are defined as

$$p_\ell(\mathbf{r}) = P_\ell(\hat{\boldsymbol{\mu}} \cdot \hat{\boldsymbol{r}}), \tag{S2}$$

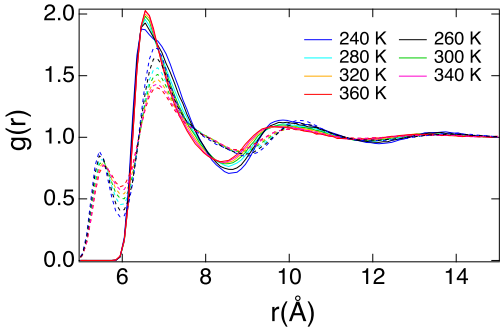

Figure S4. The radial distribution function, $g(r)$, of C_{60}^{-2} between center of fullerene and oxygen (solid lines) and hydrogen (dash lines) of water molecules for simulation trajectory 60 to 110 ns in temperature range 240-360 K.

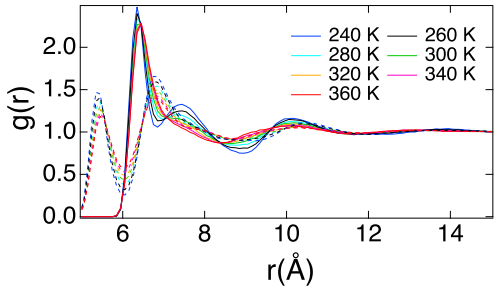

Figure S5. The radial distribution function, $g(r)$, of C_{60}^{-3} between center of fullerene and oxygen (solid lines) and hydrogen (dash lines) of water molecules for simulation trajectory 60 to 110 ns in temperature range 240-360 K.

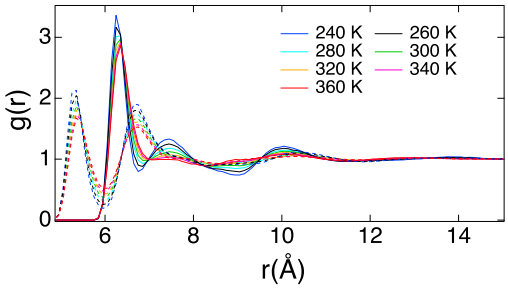

Figure S6. The radial distribution function, $g(r)$, of C_{60}^{-4} between center of fullerene and oxygen (solid lines) and hydrogen (dash lines) of water molecules for simulation trajectory 60 to 110 ns in temperature range 240-360 K.

where $\hat{\boldsymbol{\mu}}$ is unit vector of water dipole moment and $\hat{\boldsymbol{r}}$ is the radial unit vector. The orientations of two OH bonds for a given configuration of the water can be gained from the angle χ between the plane which contains the radial direction and the water dipole and the plane of the water molecule.

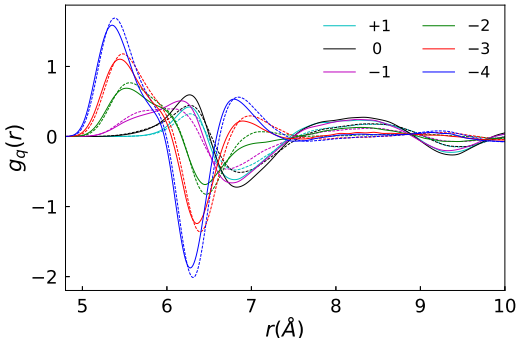

Figure S7. Distribution of water charge, $g_q(r)$ (Eq. (S1)), of C_{60}^{z} at 300 K calculated in the box with $N = 1200$ water molecules (dashed lines) and with $N = 2413$ water molecules (solid lines). The fullerene charge z is indicated in the plot.

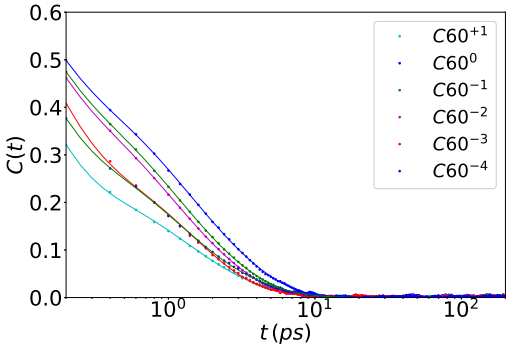

Figure S8. Time correlation functions of the first-order parameter $p_1(t)$ calculated from MD (points) and fitted to the sum of 3 exponential functions (lines, Eq. (S4)) for all charge states at 300 K.

The dynamics was studied by calculating the time auto-correlation function,

$$C_X(t) = \langle \delta X(t) \delta X(0) \rangle, \tag{S3}$$

where the dynamic variable $X(t)$ represents either the order parameter $p_1(t)$ or solute-solvent (LJ and electrostatic) interaction energies. Such correlation functions were calculated from MD trajectories for six oxidation states of fullerene and were fitted to three decaying exponents

$$S_X(t) = \frac{C_X(t)}{C_X(0)} = \sum_{n=1}^{3} A_n e^{-t/\tau_n} \tag{S4}$$

with the normalization $\sum_n A_n = 1$. Figure S8 shows the time correlation functions for the first order parameter $p_1(t)$ for $z = -4$ to 1 at 300 K. The average relaxation times were obtained according to the relation

$$\langle \tau \rangle = \sum_{n=1}^{3} A_n \tau_n. \tag{S5}$$

Their dependence on temperature was used in the Arrhenius plot (Fig. S9) to calculate the activation energies of relaxation E_a listed in Table 3 in the main text.

IV. SOLVATION THERMODYNAMICS

Convergence of the cross-correlation $\langle \delta u^{\mathrm{E}}_{0s} \delta U_{ss} \rangle$ along simulation trajectories for all charge states (+1 to −4) is shown in Fig. S10. As mentioned in the main text, the electrostatic component of solute-solvent and solvent-solvent interaction energies are calculated by extrapolating the finite-size simulation results to $N \to \infty$. All electrostatic components listed in Table 1 in the main text (e^E_{ss}, μ^E_{0s}, e^E_{0s}, e^E and Ts^E) are calculated by this approach. As an example, Fig. S11 shows the extrapolation of e^E_{ss} to the infinite-size limit. Figure S12 shows the

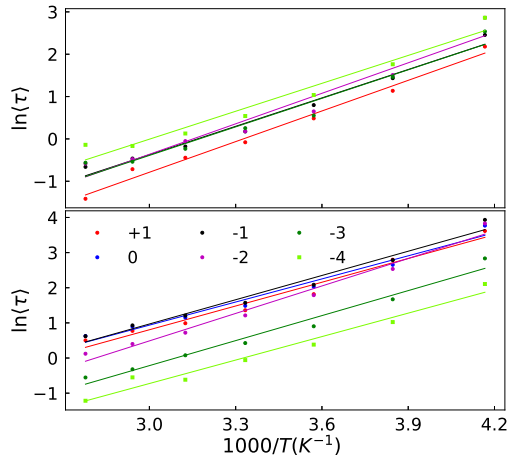

Figure S9. Average relaxation times (Eq. (S5)) for the electrostatic interaction energy in Eq. (S3) (upper panel) and for the LJ interaction energy (lower panel) vs $1/T$.

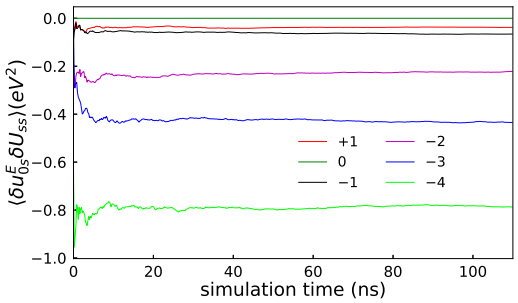

Figure S10. Convergence of the cross-correlation of the solute-solvent electrostatic energy and solvent-solvent interaction energy calculated as the running average along the 110 ns simulation trajectory at 300 K. This correlation is used to calculate the electrostatic energy of solvent restructuring e^{E}_{ss}.

electrostatic chemical potential, μ^E_{0s}, calculated by this approach as a function of the solute charge z.

V. DISTRIBUTIONS OF ORDER PARAMETERS AND ANGLE χ

The orientational structure of the first hydration layer of water at different temperatures (240-360 K) and charge states ($z = 1$ to -4) is characterized by the first-order orientational parameter (p_1), tetrahedral order parameter (Q) and the angle χ (see Fig. 1 in the main text). The average of $\langle p_1 \rangle$ was calculated for the first hydration shell. Figure S13 shows $\langle p_1 \rangle$ as a function of z at all temperatures studied by simulations. Consistent with the PDFs plots, there is a continuous decrease of $\langle p_1 \rangle$ with increasing solute charge, followed by a sharper drop for

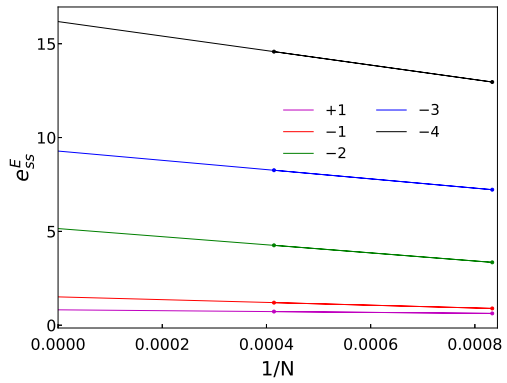

Figure S11. e^E_{ss} listed in Table 1 in the main text is calculated as extrapolating the finite-size results to $N \to \infty$ for all charge states at 300 K.

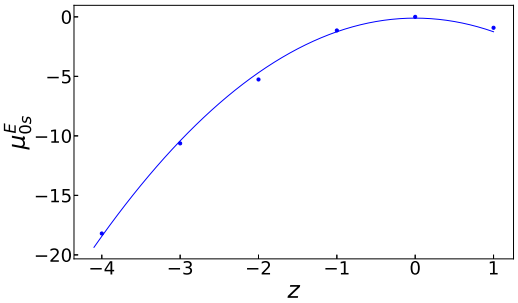

Figure S12. Electrostatic component of the solvation chemical potential as a function of the solute charge z at 300 K. The values shown by points in the plot are calculated from extrapolating the finite-size results to $N \to \infty$. The simulations are carried out in simulation boxes with $N = 1200$ and $N = 2413$ water molecules.

charge states $z = -3$ and -4. This is another manifestation of a structural crossover at $z = -3$ and $z = -4$. The distribution of p_1 for C_{60}^{-2} and C_{60}^{-3} at different temperatures are shown in Fig. S14.

As explained in the main text, the tetrahedral order parameter is calculated from the following equation

$$Q = 1 - \frac{3}{8}\sum_{i=1}^{3}\sum_{j=i+1}^{4}\left(\cos\theta_{ij} + 1/3\right)^2 . \qquad \text{(S6)}$$

where the angle θ_{ij} is the angle (i) between a water molecule and its four nearest neighbors j.

A more detailed information about the orientation of two OH bonds for a given configuration of water dipole can be gained from the angel χ. As shown in Fig. S16, the plane of the water molecule tends to orient toward to the surface of charged C_{60}^z and release the dangling OH bond.

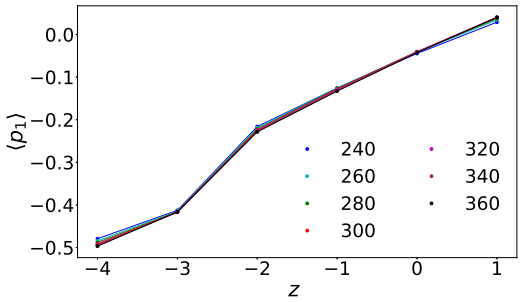

Figure S13. $\langle p_1 \rangle$ in first hydration shell of C_{60}^z as a function of charge z at different temperatures indicated in the plot.

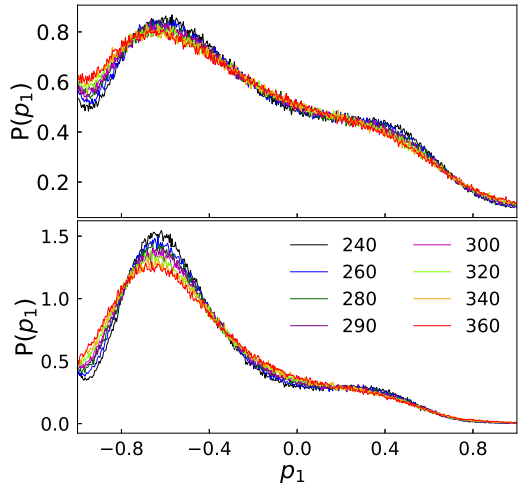

Figure S14. Distribution of the order parameter p_1 (Eq. S2) in the first hydration shell of C_{60}^{-2} (top panel) and C_{60}^{-3} (bottom panel) at various temperatures indicated in the plot. In both charge states, the maximum of $P(p_1)$ corresponds to the angle of 130° between the vector normal to the surface of C_{60}^z and water's dipole moment. Notice that the probability of p_1 at the angle of 130° is about twice higher at $z = -3$ compared to $z = -2$.

REFERENCES

[1] M. J. Frisch, G. W. Trucks, H. B. Schlegel, G. E. Scuseria, M. A. Robb, J. R. Cheeseman, G. Scalmani, V. Barone, B. Mennucci, G. A. Petersson, H. Nakatsuji, M. Caricato, X. Li, H. P. Hratchian, A. F. Izmaylov, J. Bloino, G. Zheng, J. L. Sonnenberg, M. Hada, M. Ehara, K. Toyota, R. Fukuda, J. Hasegawa, M. Ishida, T. Nakajima, Y. Honda, O. Kitao, H. Nakai, T. Vreven, J. A. Montgomery, Jr., J. E. Peralta, F. Ogliaro, M. Bearpark, J. J. Heyd, E. Brothers, K. N. Kudin, V. N. Staroverov, R. Kobayashi, J. Normand, K. Raghavachari, A. Rendell, J. C. Burant, S. S. Iyengar, J. Tomasi, M. Cossi, N. Rega, J. M. Millam, M. Klene, J. E. Knox, J. B. Cross, V. Bakken, C. Adamo, J. Jaramillo, R. Gomperts, R. E. Stratmann, O. Yazyev, A. J. Austin, R. Cammi, C. Pomelli, J. W. Ochterski, R. L. Martin, K. Morokuma, V. G. Zakrzewski, G. A. Voth, P. Salvador, J. J. Dannenberg, S. Dapprich, A. D. Daniels, . Farkas, J. B. Foresman,

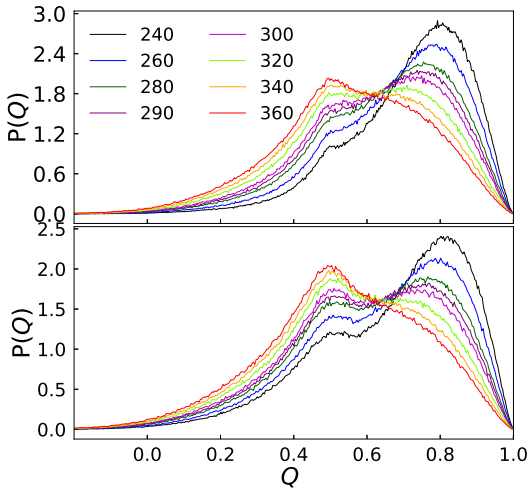

Figure S15. Distribution of the tetrahedral order parameter for C_{60}^{0} (upper panel) and C_{60}^{-2} (lower panel) at different temperatures listed in the plot.

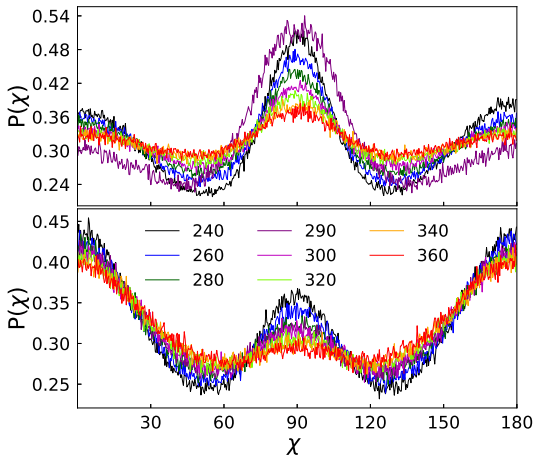

Figure S16. Distribution of the χ angle of waters in the first hydration layer of C_{60}^{-1} (top panel) and C_{60}^{-2} (bottom panel) at different temperatures.

J. V. Ortiz, J. Cioslowski, and D. J. Fox, "*Gaussian 09*, Revision E.01," Gaussian, Inc.: Wallingford, CT, 2009.
[2]J. C. Phillips, R. Braun, W. Wang, J. Gumbart, E. Tajkhorshid, E. Villa, C. Chipot, R. D. Skeel, L. Kalé, and K. Schulten, J. Comput. Chem. **26**, 1781 (2005).
[3]W. Humphrey, A. Dalke, and K. Schulten, Journal of Molecular Graphics **14**, 33 (1996).
[4]M. Dinpajooh, D. R. Martin, and D. V. Matyushov, Sci. Rep. **6**, 28152 (2016).

Table S1. Atomic charges of C_{60}^{z} in different charge states $z = +1, \ldots, -4$.

C_i	+1	0	-1	-2	-3	-4
1	0.020239	0.007413	-0.010179	0.089122	-0.078718	-0.170106
2	0.013233	-0.002965	-0.071796	-0.217126	-0.009499	-0.028600
3	0.007693	0.000292	0.008910	0.034389	0.202880	0.398406
4	0.016779	0.001313	-0.018485	-0.032333	-0.303667	-0.434081
5	0.005810	0.013777	-0.056043	-0.126347	-0.201278	-0.344196
6	0.001118	-0.022883	0.042977	0.038833	0.085595	0.136876
7	0.013691	0.013257	0.003847	-0.031127	-0.142368	-0.088290
8	0.018142	-0.020445	-0.064975	-0.159360	0.047886	-0.044095
9	0.013608	0.006099	0.051606	0.149438	-0.193011	-0.193998
10	0.017001	-0.012092	0.012797	0.058575	-0.023958	0.072180
11	0.016609	-0.015488	0.003129	0.023791	-0.178880	-0.327601
12	0.022505	-0.017887	0.018302	0.001970	0.109324	0.150697
13	0.022336	0.012865	-0.103335	-0.196721	-0.017358	-0.205573
14	0.040111	0.019065	0.033802	0.053850	-0.018168	0.067563
15	0.024206	-0.007460	0.023963	0.097831	0.111083	0.325198
16	0.035842	-0.002418	-0.048932	-0.121364	-0.111180	-0.313464
17	0.014691	0.016913	-0.026872	-0.041650	-0.060148	0.041054
18	0.013888	-0.003813	-0.064747	-0.135431	-0.086185	-0.246860
19	0.011865	-0.016725	-0.037493	-0.123713	-0.032190	-0.042611
20	0.006360	0.041274	-0.081131	-0.181348	0.078260	-0.008250
21	0.012133	-0.038124	0.066266	0.136131	-0.205127	-0.086199
22	0.008059	0.027341	0.022330	0.152371	-0.024097	-0.030710
23	0.033156	-0.008508	-0.073793	-0.286222	-0.098746	-0.256787
24	0.013082	-0.000162	0.029275	0.153163	0.014973	0.099080
25	0.046779	-0.003299	0.083422	0.164683	0.056523	0.340032
26	0.011399	-0.007750	-0.089495	-0.195699	-0.106347	-0.340786
27	0.011021	0.024341	-0.010552	-0.022691	0.007208	0.076485
28	0.005699	-0.039522	-0.012627	-0.026875	-0.195118	-0.258144
29	0.027237	0.019547	-0.027575	-0.012999	-0.032885	0.056391
30	0.013691	0.013291	0.003844	-0.031129	-0.142354	-0.088301
31	0.011865	-0.016745	-0.037491	-0.123713	-0.032202	-0.042603
32	0.013888	-0.003805	-0.064748	-0.135430	-0.086184	-0.246861
33	0.014691	0.016905	-0.026873	-0.041649	-0.060153	0.041055
34	0.001118	-0.022817	0.042974	0.038827	0.085632	0.136842
35	0.013233	-0.002887	-0.071801	-0.217132	-0.009465	-0.028636
36	0.013608	0.006069	0.051608	0.149441	-0.193024	-0.193983
37	0.018142	-0.020457	-0.064974	-0.159360	0.047884	-0.044096
38	0.006360	0.041291	-0.081133	-0.181348	0.078266	-0.008255
39	0.012133	-0.038118	0.066266	0.136131	-0.205125	-0.086204
40	0.008059	0.027341	0.022329	0.152371	-0.024089	-0.030710
41	0.013082	-0.000142	0.029274	0.153160	0.014990	0.099069
42	0.046779	-0.003341	0.083424	0.164687	0.056503	0.340051
43	0.011399	-0.007692	-0.089499	-0.195703	-0.106323	-0.340818
44	0.035842	-0.002472	-0.048928	-0.121360	-0.111205	-0.313432
45	0.024206	-0.007378	0.023957	0.097826	0.111129	0.325151
46	0.005810	0.013685	-0.056037	-0.126340	-0.201331	-0.344147
47	0.016779	0.001401	-0.018491	-0.032340	-0.303617	-0.434125
48	0.007693	0.000208	0.008915	0.034395	0.202840	0.398445
49	0.017001	-0.012072	0.012796	0.058573	-0.023949	0.072174
50	-0.004293	0.016001	-0.102593	-0.243139	-0.094821	-0.343594
51	0.016609	-0.015434	0.003125	0.023787	-0.178854	-0.327625
52	0.027237	0.019536	-0.027574	-0.012998	-0.032894	0.056396
53	0.022505	-0.017931	0.018304	0.001973	0.109298	0.150721
54	0.022336	0.012912	-0.103337	-0.196724	-0.017331	-0.205597
55	0.040111	0.018990	0.033807	0.053855	-0.018209	0.067602
56	0.005699	-0.039472	-0.012630	-0.026878	-0.195095	-0.258169
57	0.011021	0.024298	-0.010549	-0.022688	0.007190	0.076510
58	0.033156	-0.008515	-0.073792	-0.286220	-0.098760	-0.256782
59	-0.004293	0.016050	-0.102596	-0.243143	-0.094799	-0.343613
60	0.020239	0.007344	-0.010175	0.089127	-0.078750	-0.170076